Progress In Electromagnetics Research, Vol. 135, 215–229, 2013

A VARIABLE PRF IMAGING METHOD FOR HIGH SQUINT DIVING SAR

Huaping Xu*, Jing Gao, and Jianlong Li

School of Electronic and Information Engineering, Beihang University, Beijing, China

Abstract—The high squint diving SAR is widely used to provide the information in advance. Large squint angle deduces the deeper coupling of range and azimuth of SAR echoes which makes SAR imaging more difficult. Especially, the large range migration of the deep couple heavily burdens the imaging processing time and storage units. The diving motion of platform worsens the situation. This paper proposes the varied azimuth sample frequency (Pulse Repeat Frequency, PRF) to implement the high squint diving SAR imaging. Based on the signal model of the diving squint SAR, it is analyzed that the range walk is the prominent component of range migration in the high squint SAR. The varied PRF imaging method dramatically decreases the range walk of echoes by shifting the beginning position of transmitted pulses and received echoes and the shift is implemented by the PRF variation. Then the range migration is decreased and the couple of range and azimuth of SAR echoes is reduced. The PRF variation law is deduced and the applicable condition of varied PRF is presented. The simulation results show that the variable PRF method is efficient to reduce range walk of echoes. Comparison to the traditional constant PRF, the novel variable PRF method for high squint needs less storage and less time expense, which is helpful to real time SAR imaging. The non-uniform FFT can be used for the azimuth compressing of the variable PRF SAR. It will simplify the implementation of the variable PRF SAR imaging.

1. INTRODUCTION

Synthetic aperture Radar (SAR) is widely used in many fields because of its all-weather, day-or-night capability. It receives the raw echoes

Received 23 November 2012, Accepted 14 December 2012, Scheduled 19 December 2012
* Corresponding author: Huaping Xu (xuhuaping@buaa.edu.cn).

of radar signals and provides the high resolution SAR imagery by complex imaging process [1]. Usually, SAR transmits the Chirp Scaling pulses and receives the backscatter echoes in broadside mode which the SAR antenna is pointed 90° with respect to the velocity vector of the platform. In some cases, the SAR antenna is pointed with an angle offset from the perpendicular direction to the motion of the platform. The angle offset is called squint angle [2]. The high squint SAR with large squint angle is used to obtain some unavailable information in broadside mode or to provide the information in advance. The squint SAR has provided natural disaster environment information to the rescues and reconnaissance and surveillance information to military operations. For these applications, the diving high squint SAR imaging is usually required, such as missile-borne SAR guidance.

The high squint angle and the diving of platform motion lead to the deeper coupling of range and azimuth of SAR echoes which makes SAR imaging more difficult. It behaves larger range migration and larger variation in the Doppler Centroid as a function of range [3, 4]. Range walk is the linear component of the range migration through range cells, which makes the azimuth information of one target be dispersed over many range units and SAR azimuth compression be 2-dimensional processing. Large range walk needs more memory units and more processing time in SAR imaging. Large variation of the Doppler Centroid requires the imaging parameters varying with range which also slows the processing.

The current researches are mainly focused on improving the exiting SAR imaging algorithms to deal with the coupling problem of range and azimuth in high squint SAR mode and to implement precise high squint SAR imaging. It is shown that Range Doppler (RD) algorithm is not precise enough to focus squint SAR signal in high squint angle situation [5]. Chirp Scaling algorithm [6] is favored to high squint SAR imaging. Extended chirp scaling algorithm is proposed to process the high squint SAR data in [7]. It introduces a cubic phase term to focus squint SAR echoes and accommodates the variations of the Doppler Centroid. [8] presents an improved CS imaging algorithm which removes range walk in time domain for high squint SAR. [9] refines the signal model of classic CS algorithm to implement precisely imaging in high squint. [10] improves the nonlinear chirp scaling algorithm to correct the range migration in the 2-dimenstion frequency and to compensate the azimuth variation of Doppler parameters. [11] corrects the range walk firstly and then employs the modified azimuth nonlinear chirp scaling to overcome the parameters variation.

The wavenumber domain algorithm, also called as range migration

algorithm, is one kind of accurate algorithm for high squint SAR imaging [4, 12–14]. The modified stolt mapping is introduced to enlarge the range extension and to update the Doppler parameters in [4]. [13] modifies a reference signal based on the Taylor approximation and the coordinate transformation and transforms the squint mode echoes to a broadside-mode echoes. The extended wavenumber domain algorithm is presented for the squint SAR motion error compensation in [14]. Sub aperture technique also is used to the high squint SAR. [5] divides the received SAR signal into the sub apertures in azimuth and develops a new subaperture approach to high squint SAR Processing. The large range walk problem is avoided because each subaperture is corresponding to a small part of the total signal. Using sub aperture method, the improved step transform algorithms are developed for highly squint stripmap SAR imaging in [15, 16]. Polar format algorithm (PFA) [17, 18] is a kind of precise SAR imaging algorithms. But it is only suitable for the SAR in small squint angle.

As mentioned above, all of the documents about the high squint SAR imaging endeavor to improve the SAR image processing. So SAR imaging algorithms are more and more complicated. It heavily burdens the SAR imaging storage units and processing time. This paper proposes varied azimuth sample frequency (Pulse Repeat Frequency, PRF) to implement the high squint SAR imaging. The varied PRF is firstly presented to deal with the conflict between high resolution and wide-swath and to achieve the high resolution and ultra-wide swath SAR imaging [19, 20]. Conventional SAR system operates on a constant PRF. The SAR antenna transmits the pulses and receives the echoes by the same PRF in one imaging scene [21–23]. For the variable PRF SAR system, the sample frequency is varying with the azimuth. Blind ranges of SAR system with varied PRF SAR in [19, 20] disappear and the swath width is no longer limited by the applied PRF.

This paper employs the varied PRF to decouple the range and azimuth of high squint SAR echoes. The range walk is removed or decreased dramatically in this case. Non uniform FFT [24–27] is only needed to implement the variable PRF SAR imaging but not complicated SAR imaging algorithm to decouple the range and azimuth for high squint SAR. The characteristics of high squint diving SAR are analyzed and the varying rules of PRF are presented in this paper. The variation of PRF is implemented by shifting the starting positions of transmitted pulses and received echoes. Then the range walk of echoes is depressed which can simplify imaging algorithm. The novel imaging method for the high squint SAR needs less storage and less time expense, which is helpful to the real time SAR imaging.

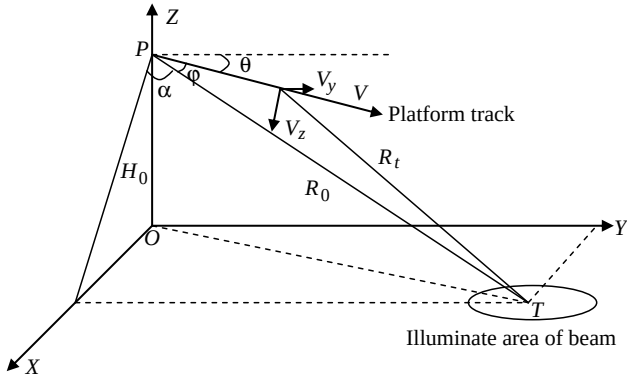

Figure 1. Equivalent range model of high squint diving SAR.

2. RANGE MIGRATION OF HIGH SQUINT DIVING SAR

Figure 1 shows the geometric relation of the high squint diving SAR, where H_0 is the initial platform height; platform dives in a speed V; V_y is the horizontal speed; V_z is the vertical speed; α is the squint angle of SAR imaging; φ is the angle between beam centre and platform motion direction, defined as equivalent squint angle; θ is the angle between horizontal speed and resultant speed of platform, defined as trajectory inclination angle; R_0 is the reference slant range between platform and target at the initial time; R_t is instantaneous slant range at time t; P is the starting point of the motion, and T is point target on the ground.

From Figure 1, instantaneous slant range equation between platform and target is given as

$$R_t = \sqrt{R_0^2 + (Vt)^2 - 2R_0 Vt\cos\varphi} \tag{1}$$

Expanding Equation (1) into Taylor polynomial series at $t = 0$, it is obtained that

$$R_t = R_0 + (-V\cos\varphi)t + \frac{V^2\sin^2\varphi}{2R_0}t^2 + \dots \tag{2}$$

Calculate the range migration ΔR,

$$\Delta R = R_t - R_0 = (-V\cos\varphi)t + \frac{V^2\sin^2\varphi}{2R_0}t^2 + \dots \tag{3}$$

The linear term on right side of the equality in Equation (3) is the range walk. The quadratic term is the range curvature. Usually the

Table 1. System parameters of diving SAR.

Height	20000 m
Incident angle	30°
Squint angle	5°, 30°, 70°
Horizontal speed	2000 m/s
Vertical speed	2500 m/s
Wavelength	0.03 m
Antenna aperture	1 m

Table 2. The maximum variation of range migration (5°, 30°, 70°).

Range migration (m)	5°	30°	70°
The first order term: range walk	101.73	230.95	340.55
The second order terms: range curvature	6.36	1.25	0.03
The third and higher order terms	0.0104	0.0108	1.47×10^{-4}

terms of more than three exponents could be neglected. So the range migration can be approximately decomposed into range walk and range curvature.

In order to investigate the effect of large squint angle on echoes, the migration is calculated in case of the SAR parameters as Table 1.

Simulating range variation of the point target in the parameters shown as Table 1, we can obtain respectively the quantity of different terms of range migration in 5°, 30°, 70° squint angles shown in Table 2.

It is shown that the range walk increases with the squint angle while the range curvature decreases. An obvious range curve can be found in 5° squint angle, but the range migration becomes almost a straight line when the squint angle increases to 30°, and especially 70°. So range migration is mainly caused by the range walk in the large squint angle. It is the range walk that needs only to be suppressed in the larger squint angles for SAR imaging.

3. THE VARIABLE PRF IMAGING METHOD OF HIGH SQUINT DIVING SAR

Diving SAR is required to be able to image in high squint for collecting information ahead such as the missile-borne SAR. The large quantity of echoes data and the obvious range migration make it a great challenge

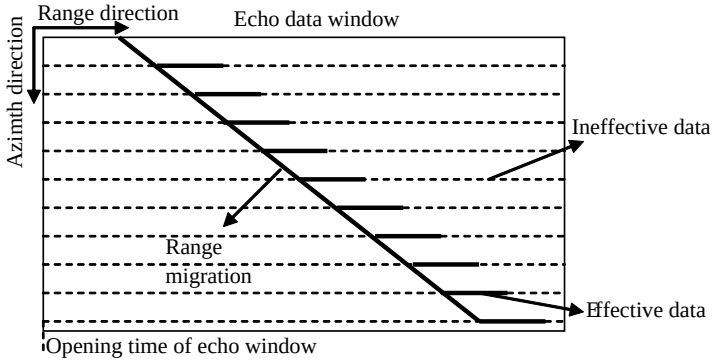

Figure 2. The schematic diagram of echoes in high squint.

to store information and to image in real-time. The diagram of echo data in high squint of diving SAR is given in Figure 2 where dashed line is ineffective data and horizontal black solid line is effective data. One point target echoes are shown in Figure 2. The echoes of every resolution cell in the ground are recorded in two dimensional. The size of azimuth dimension is determined by the synthetic aperture time. The size of range dimension is determined by the pulse width and the range migration. If the range migration is very small, the size of range dimension of the echoes is nearly equivalent to the pulse width which is the size of the effective data. But for the high squint, the size of range dimension of the echoes is the addition of range size of the effective data and the size of range migration. With the increase of the range migration, the more and more ineffective data, marked as dash line in Figure 2, are included in the echo window. The larger squint angle leads to the larger range migration which makes the echo window full of a larger number of ineffective data and causes the waste of storage space and imaging time.

It is shown as in Section 2 that the range walk gets more and more obvious with the squint angle increasing while the influences of range curvature and the higher terms, however, become fainter. Therefore, it is only demanded to compensate range walk in large squint angle to greatly decrease range migration.

3.1. The Imaging Principle of Variable PRF SAR

In order to solve the imaging problem of diving SAR in large squint angle, this paper proposes the non-uniform sampling imaging method in azimuth by PRF variation. Through the variation of PRF in azimuth direction, the echoes receiving windows are shifted to filter

the majority of ineffective data to decrease the range walk of echoes. So the storage space needed by echo data is saved and the imaging time is reduced which will benefit real-time imaging processing. The diagram of variable PRF principle is given as Figure 3 where black solid line is the transmitted pulse and received echoes with constant PRF and black dashed line is the pulse and echoes with variable PRF. In this figure, τ is the pulse width, τ_p is the time interval from the end of transmitted pulse to the open time of echo window, $1/prf_0$ is the pulse repetition period for constant PRF, $1/prf_k$ is the pulse repetition period corresponding to the kth change of variable PRF. It is known that echoes corresponding to the transmitted pulse can be received at least one pulse period [28, 29]. So it is supposed that every echo passes one pulse period before it is received. T_1 is the time interval of constant PRF which is from the pulse being transmitted to being received. T_2 is the time interval of variable PRF.

The key point of variable PRF imaging method is to compensate the range walk by changing the opening time of the echo window and to implement the opening time shift by PRF variation. For high squint diving SAR, the range of a point target is variable with the azimuth time. The opening time of the receiving window should be shifted to guarantee that the echoes of the same target at every azimuth time start from the same range gate during the whole synthetic aperture T_{syn}. Suppose $R_W(t)$ is the range walk during time t, then

$$R_W(t) = \frac{c \cdot \Delta T}{2} \tag{4}$$

where c is the light velocity, ΔT is the overall time shift of the PRF. Because of the linearity of the range walk, then

$$R_W(t) = \frac{c \cdot n\Delta prt}{2} \tag{5}$$

where Δprt is the pulse repeat time increment, n is the number of pulses during t.

As shown in Figure 3, variable PRF method opens the echo window with time shift to filter ineffective data and obtain echo data with smaller range migration. Figure 4 compares the echoes obtaining with the constant PRF and the variable PRF. Bolded solid line is the range migration curve of constant PRF, while the bolded dashed line is the range migration curve of variable PRF. The two kinds of oblique dashed lines respectively represent effective data obtained by the traditional constant PRF method and the variable PRF method. The vertical dashed curve on the left side is the echo window opening time of variable PRF. It is fixed of echo window opening time by traditional constant PRF method, but the receiving echoes delay time

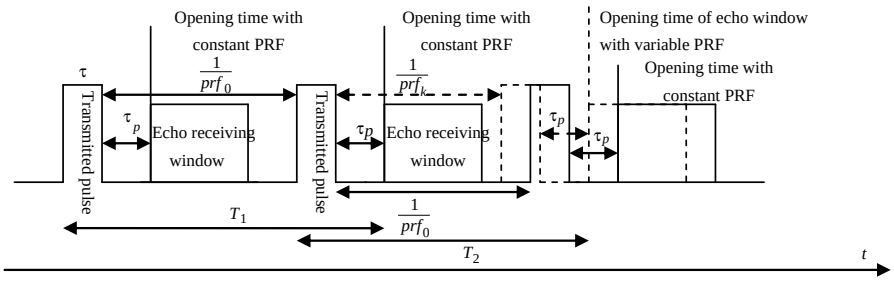

Figure 3. Variable PRF imaging principle.

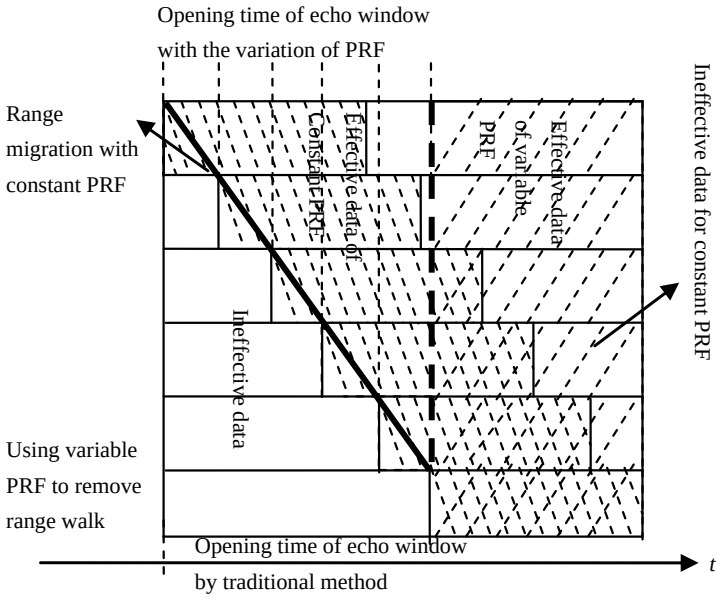

Figure 4. Echoes with traditional and variable PRF imaging method.

increases with the increasing of distance from radar to target. Thus range migration comes into being. Furthermore, with the increasing of squint angle, the change of slant range becomes larger, followed by the increasing range migration. Echo window opening time is shifted according to the range variation and ineffective data is filtered by variable PRF imaging method. It leads to the initial range gate of effective echoes in different azimuth position to be approximately same, and to reduce the range migration. The storage space required by traditional constant PRF method not only contains the samples in

a pulse width, but also stores the samples between the largest slant range interval, which obviously needs a larger storage space. As for the variable PRF imaging method, however, the shifting echo window filters ineffective data and the effective data is only received. So storage space only contains the samples in one pulse width. Furthermore, because of the strict linearity of range walk, it is realizable to remove range walk with the variation tendency of PRF. It is significant to image in high squint diving SAR.

3.2. The PRF Variation Law for Reducing Range Walk

In this paper, calculation of the PRF variation law is implemented by using the large squint angle equivalent range model of diving SAR shown in Figure 1, principle of variable PRF shown in Figure 3, instantaneous slant range formula shown as Equation (1) and Taylor polynomial series shown as Equation (2). From Equation (2), range walk within time t is

$$R_W(t) = -V\cos\varphi \cdot t \tag{6}$$

Supposing that the first pulse in Figure 3 is transmitted at reference position, then

$$T_1 = \frac{2R_0}{c} = \frac{1}{prf_0} + \tau + \tau_p \tag{7}$$

$$T_2 = \frac{2\left(R_0 + R_W\left(\frac{1}{prf_0}\right)\right)}{c} = \frac{2\left(R_0 - V\cos\varphi\frac{1}{prf_0}\right)}{c} = \frac{1}{prf_1} + \tau + \tau_p \tag{8}$$

Using Equation (4) and (5), subtract the two equations above, then

$$\frac{2V\cos\varphi\frac{1}{prf_0}}{c} = \frac{1}{prf_0} - \frac{1}{prf_1} \tag{9}$$

Because the range walk is linear, the increment of PRF is constant and is written as Δprf. Then

$$prf_1 = prf_0 + \Delta prf \tag{10}$$

Δprf is calculated as

$$\Delta prf = \frac{2V\cos\varphi prf_0}{c - 2V\cos\varphi} \tag{11}$$

The variation law of azimuth PRF is deduced by

$$prf_k = prf_0 + k\Delta prf \tag{12}$$

where prf_k is the PRF of kth transmitted pulse.

For the high squint diving SAR, PRF linearly increases with the motion of platform. Because of the linearity of range walk in time domain, the echo window opening time shift can be calculated by equivalent slant range and slant range difference. This opening time suits to whole synthetic aperture time.

3.3. The Applicable Condition of Variable PRF Imaging Method

It is no doubt that the echoes with smaller range migration can be obtained by variable PRF imaging method. But there is an applicable condition. The condition is that the received echoes have to be delayed at least one pulse compared to the transmitted pulse. It can also be seen in principle diagram as Figure 3. If the echo of one transmitted pulse is received before the emission of the next pulse, it is no meaning to change the opening time of echo receiving window with variable PRF. The applicable condition is

$$\frac{2R_n}{c} > \frac{1}{prf_0} \tag{13}$$

where R_n is the nearest slant range and prf_0 the pulse repetition frequency. As for missile-borne SAR, PRF is over 10000 Hz, the height in cruise stage about 15000–20000 m, and the nearest slant range larger than operational height in slant mode. Substituting height and PRF into Equation (13), the calculation result meets the requirement. For missile-borne SAR platform, it is feasible to obtain echoes with small range migration in large squint angle by using variable PRF method.

4. COMPUTER SIMULATING AND RESULTS ANALYSIS

Using variable PRF imaging method, simulate the diving SAR echoes. The simulation parameters are given in Table 1. PRF =8000 is used as a supplementary parameter. The simulated squint angle is respectively 5° and 70°. Simulated point target is set as: 2 points in azimuth direction with 100 m space and 3 points in range direction with 500 m space. Using Equation (13), we have $\frac{2\times 20000}{3\times 10^8} > \frac{1}{8000}$, which satisfies applicable condition.

Figure 5 and Figure 6 show the simulated echoes of two kinds of squint angles. Figure 5(a) and Figure 6(a) give the echoes of the traditional constant PRF method. Figure 5(b) and Figure 6(b) are the 2-dimensional spectrum of the constant PRF. Figure 5(c) and Figure 6(c) are the echoes obtained with the variable PRF

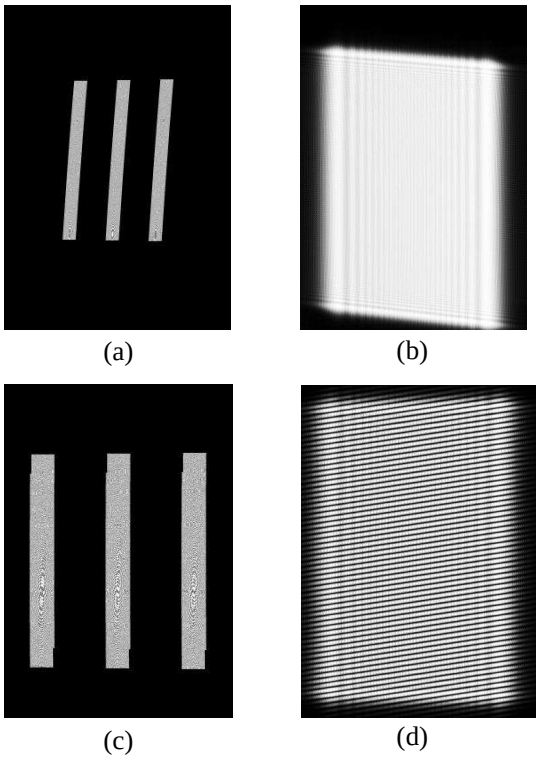

Figure 5. Comparison of echoes and spectrum (squint angle = 5°). (a) Echoes with constant PRF. (b) 2-dimensional spectrum with constant PRF. (c) Echoes with variable PRF. (d) 2-dimensional spectrum with variable PRF.

method. Figure 5(d) and Figure 6(d) show 2-dimensional spectrum of the variable PRF. Table 3 gives the numerical comparison of range migration by the two methods.

From the simulation results, it is shown that the range migration is large with the constant PRF when the squint angle is large. It needs more storage space and leads to much deeper range and azimuth couple of two-dimensional spectrum. These characteristics will bring difficulties to SAR imaging. The variable PRF method put forward in this paper can remove the range walk which is the prominent part of range migration in large squint angle. The echoes quantity reduces 8 times in this simulation which saves the storage space in large squint angle. For small squint angle, here also exists range migration in some degree in echoes because of the range curvature after the removal of range walk.

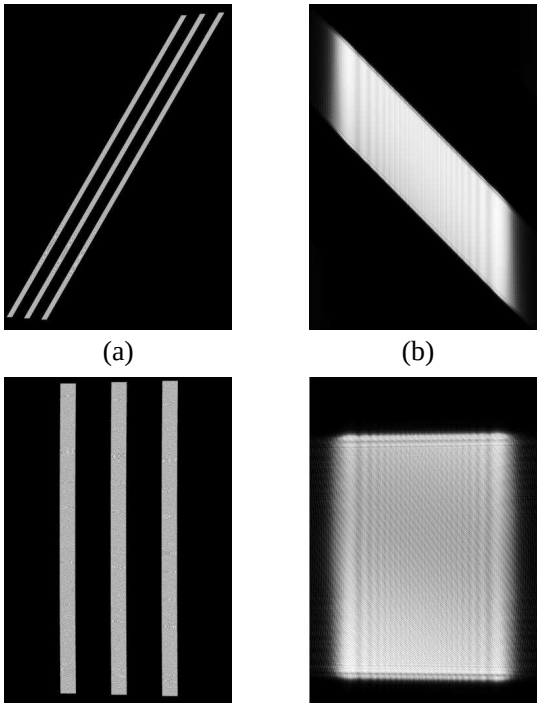

Figure 6. Comparison of echoes and spectrum (squint angle = 70°). (a) Echoes with constant PRF. (b) 2-dimensional spectrum with constant PRF. (c) Echoes with variable PRF. (d) 2-dimensional spectrum with variable PRF.

Table 3. The numerical comparison of range migration of two methods.

Squint angle	5°	70°
Range migration	108.1 m	340.58 m
The number of range gates	37	514
Corrected range migration	6.37 m	0.031 m
The number of range gates after correction	3	0

5. CONCLUSION

In order to implement high solution and wide width SAR imaging and obtain information in advance, diving high squint SAR mode is applied.

But the deeper couple of range and azimuth appears in the mode. Large range migration of deep couple SAR echoes highly restricts the speed and correctness of SAR imaging. This paper analyzed the characteristic of range migration in large squint angle and put forward a novel variable PRF method to remove range walk in large squint angle mode. The echoes of the variable PRF SAR is acquired with little range migration and can be compressed in azimuth with non-uniform FFT. So the signal storage space is saved and the image process is speeded. The results of simulation proved the effectiveness of this method.

But there is an applicable condition for the proposed method. It is that the received echoes have to be delayed at least one pulse compared to the transmitted pulse. Also the applicable condition is analyzed quantificationally in this paper.

ACKNOWLEDGMENT

The authors would like to thank the anonymous reviewers for their valuable comments and useful suggestions. This work was supported by the National Natural Science Foundation of China under contract No. 60901055.

REFERENCES

1. Xu, W., P. P. Huang, and Y.-K. Deng, "Multi-channel SPCMB-tops SAR for high-resolution wide-swath imaging," *Progress In Electromagnetics Research*, Vol. 116, 533–551, 2011.
2. Park, S.-H., J.-I. Park, and K.-T. Kim, "Motion compensation for squint mode spotlight SAR imaging using efficient 2D interpolation," *Progress In Electromagnetics Research*, Vol. 128, 503–518, 2012.
3. Chang, C. Y., M. Jin, and J. C. Curlander, "Squint mode SAR processing algorithms," *IGARSS' 89*, 1702–1706, Vancouver, 1989.
4. Guo, D. M., H. P. Xu, and J. W. Li, "Extended wavenumber domain algorithm for highly squinted sliding spotlight SAR date processing," *Progress In Electromagnetics research*, Vol. 114, 17–32, 2011.
5. Yeo, T. S., N. L. Tan, C. B. Zhang, and Y. H. Lu, "A new subaperture approach to high squint SAR processing," *IEEE Trans. Geosci. Remote Sens.*, Vol. 39, No. 5, 22–36, 2001.
6. Chen, J., J. Gao, Y. Zhu, W. Yang, and P. Wang, "A novel image formation algorithm for high-resolution wide-swath spaceborne

SAR using compressed sensing on azimuth displacement phase center antenna," *Progress In Electromagnetics Research*, Vol. 125, 527–543, 2012.

7. Moreira, A. and Y. Huang, "Airborne SAR processing of highly squinted data using a chirp scaling approach with integrated motion compensation," *IEEE Transaction on Geoscience Remote Sensing*, Vol.32, No. 5, 1029–1040, 1994.
8. Wu, Y., H. J. Song, and J. Peng, "Chirp scaling imaging of SAR in high squint mode based on range walk removal," *Journal of Electronics & Information Technology*, Vol. 32, No. 3, 593–598, 2010.
9. Ding, Z. G., T. Long, et al., "Highly squint airborne SAR real-time imaging," *IEEE Proceedings*, 1–4, 2006.
10. Zhou, S., M. Bao, et al., "An imaging algorithm for missile-borne SAR with downward movement based on azimuth nonlinear chirp scaling, " *Journal of Electronics & Information Technology*, Vol. 33, No. 6, 1420–1426, 2011.
11. An, D. X., Z.-M. Zhou, X.-T. Huang, and T. Jin, "A novel imaging approach for high resolution squinted spotlight SAR based on the deramping-based technique and azimuth NLCS principle," *Progress In Electromagnetics Research*, Vol. 123, 485–508, 2012.
12. Li, S. Y., B. Ren, H.-J. Sun, W. Hu, and X. Lv, "Modified wavenumber domain algorithm for three-dimensional millimetre-wave imaging," *Progress In Electromagnetics Research*, Vol. 124, 35–53, 2012.
13. Shin, H. S. and J. T. Lim, "Range migration algorithm for airborne squint mode spotlight SAR imaging," *IET Radar Sonar Navigation*, Vol. 1, No. 1, 77–82, 2007.
14. Deng, Y. K. and G. W. Tan, "Squint SAR data processing with extended wavenumber domain algorithm combines motion compensation, " *IEEE Proceedings,* 1–4, 2008.
15. Sun, X. B., T. S. Yeo, et al., "Time-varying step-transform algorithm for high squint SAR imaging," *IEEE Transactions on Geoscience and Remote Sensing*, Vol. 37, No. 6, 2668–2677, 1999.
16. Li, W. and J. Wang, "A new improved step transform algorithm for highly squint SAR imaging," *IEEE Geoscience and Remote Sensing Letters*, Vol. 8, No. 1, 118–122, 2011.
17. Liu, Q., W. Hong, W. Tan, Y. Lin, Y. Wang, and Y. Wu, "An improved polar format algorithm with performance analysis for geosynchronous circular SAR 2D imaging," *Progress In Electromagnetics Research*, Vol. 119, 155–170, 2011.

18. Wang, Y., J. Li, J. Chen, H. Xu, and B. Sun, "A novel non-interpolation polar format algorithm using non-lineal flight trajectories and auto-adaptive PRF technique," *Progress In Electromagnetics Research*, Vol. 122, 155–173, 2012.
19. Krieger, G., M. Younis, et al., "Advanced concepts for high-resolution wide-swath SAR imaging," *EUSAR 2010*, 524–527, 2010.
20. Gebert, N. and G. Krieger, "Ultra-wide swath SAR imaging with continuous PRF variation," *EUSAR 2010*, 966–969, 2010.
21. Ren, X.-Z., L. H. Qiao, and Y. Qin, "A three-dimensional imaging algorithm for tomography SAR based on improved interpolated array transform1," *Progress In Electromagnetics Research*, Vol. 120, 181–193, 2011.
22. Li, S., H. Xu, and L. Zhang, "An advanced DSS-SAR insar terrain height estimation approach based on baseline decoupling," *Progress In Electromagnetics Research*, Vol. 119, 207–224, 2011.
23. Ma, L., Z.-F. Li, and G. Liao, "System error analysis and calibration methods for multi-channel SAR," *Progress In Electromagnetics Research*, Vol. 112, 309–327, 2011.
24. Fessler, J. A. and B. P. Sutton, "Nonuniform fast Fourier transforms using min-max interpolation," *IEEE Transactions on Signal Processing*, Vol. 51, No. 2, 560–574, 2003.
25. Subiza, B., E. Gimeno-Nieves, et al., "Non-uniform FFT's (NUFFT) algorithms applied to SAR imaging," *SAR Image Analysis, Modelling, and Techniques VI, Proceedings of SPIE*, Vol. 5236, 72–79, 2004.
26. Wang, Q. Z. and W. T. Lei, "A novel NUSS-FFT SAR imaging algorithm of non-uniform spatial sampling data," *IEEE Proceedings*, 3795–3798, 2011.
27. Huang, Y., Y. Liu, Q. H. Liu, and J. Zhang, "Improved 3-D GPR detection by NUFFT combined with MPD method," *Progress In Electromagnetics Research*, Vol. 103, 185–199, 2010.
28. Liu, Y., Y.-K. Deng, R. Wang, and X. Jia, "Bistatic FMCW SAR raw signal simulator for extended scenes," *Progress In Electromagnetics Research*, Vol. 128, 479–502, 2012.
29. Liu, Q., W. Hong, W. Tan, and Y. Wu, "Efficient geosynchronous circular SAR raw data simulation of extended 3-D scenes," *Progress In Electromagnetics Research*, Vol. 127, 335–350, 2012.